

Mechanisms of Hydrogen Embrittlement During Low Cycle Fatigue in Metastable Austenite

M. LABIDI*, M. HABASHI* M. TVRDÝ** and
J. GALLAND*

*Ecole Centrale des Arts et Manufactures,
92295 Chatenay-Malabry, France

**Research Institut of Vitkovice, Ostrava, Czechoslovakia

ABSTRACT

This paper deals with the effect of cathodic hydrogen charging on the low cycle fatigue LCF behaviour in an austenitic Fe-23%Ni-0.4%C alloy. The results point out that this alloy is hardened during cycling, due to the formation of strain - induced and stress-assisted martensites. Hydrogen embrittlement is high and is calculated by taking $\left\{ 1 - \frac{(2N \Delta \epsilon_p)_{\text{hydrogen}}}{(2N \Delta \epsilon_p)_{\text{air}}} \right\}$ as a criterion to this embrittlement ($2N \Delta \epsilon_p$ is the cumulative plastic strain with N number of reversal cycles and $\Delta \epsilon_p$ plastic amplitude). Cyclic strain hardening exponent is lowered by the presence of hydrogen. It is thought that $\gamma \rightarrow \alpha'$ transformation is responsible for hydrogen embrittlement in the range of plastic strain levels investigated.

INTRODUCTION

Many papers have shown that metastable austenitic steels were transformed entirely or partially, depending on their chemical compositions and on the test temperature, to martensite during monotonic tensile and fatigue tests (1, 2, 3, 4) and their mechanical properties were strongly affected. The cyclic stress - strain curve (CSSC) is one of the most important properties of materials under repeated loading. Such a curve is obtained by connecting the tips of stable hysteresis loops for comparable specimens tested at different strain amplitudes. The relation between stress amplitude $\Delta \sigma / 2$ and plastic strain amplitude, $\Delta \epsilon_p / 2$ can be expressed by a power function of the form used for the monotonic curve :

$$\Delta \sigma / 2 = K' (\Delta \epsilon_p / 2)^{n'} \quad (1)$$

where K' and n' are the cyclic strength coefficient and cyclic strain hardening exponent, respectively. The main reasons for measuring these parameters and others issued from the MANSION - COFFIN curves, S - N curves etc... is to enable the calculation of martensite transformations on the fatigue behaviour in metastable austenitic steels were studied (4, 5, 7) in the

range of temperatures higher than either M_S or M_D or between these two temperatures. The results show that at a given plastic strain amplitude, the formation of α' martensite leads to substantial cyclic hardening of the material and to a decrease of its fatigue life (4). The $\gamma \rightarrow \alpha'$ transformation occurs when the temperature is lower than M_D and when $\Delta E_p/2$ is larger than a critical value which increases when the test temperature increases in the temperature range between M_S and M_D (4).

On the other hand, the LCF life of a TRIP steel both at room temperature or at 200°C (no $\gamma \rightarrow \alpha'$ transformation) is related to plastic strain range by the following relationship (5) :

$$\Delta E_p \cdot N_f^{1/2} = C = 1/2 (\epsilon_f - \epsilon_0) \quad (2)$$

where N_f (LCF life) and C (constant) are depending on monotonic fracture strain ϵ_f and ϵ_0 , pre-strain amplitude.

All the previous studies had been performed in air, neglecting the effects of an aggressive environment, such as the diffusion of hydrogen in the material during LCF. The aim of this work is to point out the effect of hydrogen diffusion during LCF process on $\gamma \rightarrow \alpha'$ transformation in an austenitic metastable alloy Fe-23%Ni-0.4%C.

EXPERIMENTAL PROCEDURE

The chemical composition of the alloy which was used is given in table I.

Table I : Chemical composition of the Fe-Ni-C alloy (% wt)

C	Mn	Si	P	S	Ni
0.38	0.48	0.29	0.022	0.017	23.68

Annealing of one hour at 1050°C followed by water quenching was applied. The final grain size was approximately 70 μm . The M_S ($\gamma \rightarrow \alpha'$) temperature of this alloy is -55°C. The M_D temperature is not yet determined. Experiments were carried out on cylindrical fatigue specimen having 7 mm of diameter and 12 mm of gauge length and tested under fully reversed strain - controlled conditions in a hydraulic servovalve MTS machine, using longitudinal extensometer, triangular wave form and cyclic frequency equal to 0.05 Hz. Cathodic hydrogen charging was performed using half cylindrical micro-cell sticked to the specimen, on the opposite side of the extensometer. A cathodic potential of -1.5 V/ESS in H_2SO_4 1N acid was employed to achieve hydrogen charging. Immediately after failure, the hydrogenated specimens were quenched in liquid nitrogen for further outgassing under vacuum at 600°C to enable the determination of the quantity of hydrogen introduced during LCF tests. In all tests, the mean strain was maintained at zero level. Tests were conducted at room temperature (20°C).

RESULTS

MANSON and al. (6) have shown that a metal resistance to total strain cycling can be considered as the summation of its elastic and plastic

strain resistances : $\Delta E_t/2 = (\Delta E_e/2) + (\Delta E_p/2) = (\sigma_f'/E)2N_f^b + \epsilon_f'(2N_f)^c$ where σ_f' and ϵ_f' are true monotonic fracture strength and true monotonic fracture strain, respectively. b and c respectively are the fatigue strength exponent and fatigue ductility exponent. E and N_f are the elastic modulus and the fatigue life, respectively. Strain hardening exponent n' may be deduced by the relationship : $n' \approx (b/c)$ (7).

In the following, we are going to study the effect of hydrogen on the elastic and plastic strain resistances as a function of fatigue life. Figures 1a and 1b show that cathodic hydrogenation reduces both strain resistances. However, the plastic strain resistance is more affected, especially at lower plastic strain amplitude. Moreover, the fatigue ductility exponent C is higher when the alloy is hydrogen charged than when calculated for the case of the material tested in air as it could be observed on the following numerical values :

Enviroment	$\Delta E_e\%$	b	$\epsilon_f\%$	c
Air	1.48	-0.12	27.68	-0.62
Hydrogen	0.88	-0.12	24.33	-0.47

The summation of the elastic and plastic strain resistances ($\Delta E_t/2$) shows that hydrogen also reduces the fatigue life in the range of ΔE_t levels investigated, figure 1c. Cyclic strain hardening exponent n' is calculated from the stress - strain hysteresis recorded at half fatigue life and compared with the results of the previous relationship, table II.

Table II : n' values according to b/c relationship, and hysteresis recorded at $N_f/2$ with and without hydrogen

Air	Hydrogen	n'
0.245	0.187	from b/c
0.195	0.126	from hysteresis at $N_f/2$

It is obvious that hydrogen charging reduces the life time and also the cyclic strain hardening exponent n' . Its absolute values are different depending on the way this parameter is calculated. n' is usually measured at stabilized cyclic stress - strain hysteresis when $N = N_f/2$, figures 2a and 2b. The alloy is hardened by increasing the cumulative plastic strain $2N\Delta E_p$, independently of the plastic strain amplitude and hydrogen charging. Plotting the cumulative plastic strain versus plastic strain amplitude, figure 3, we observe that there is a great reduction of the cumulative plastic strain when the material is cathodically charged. From this figure we can calculate the reduction ratio at each plastic strain level and take it as criterion to hydrogen embrittlement in LFC tests and is designated by us as $F_c\%$: the cyclic index of hydrogen embrittlement and is equal to $\{1 - [(2N\Delta E_p)_{\text{hydrogen}} / (2N\Delta E_p)_{\text{air}}]\}$. Figure 4 shows that F_c decreases from 95% to about 75% when the plastic strain amplitude is increased from 0.16% to 2%. Plotting the quantity of hydrogen desorbed at 600°C Q_H as a function of $\Delta E_p\%$, we observe a large scattering but the trend also shows that Q_H is a decreasing function of the increasing ΔE_p

DISCUSSION

The results obtained in this work are in good agreement with those found by other authors (3, 4). That is to say, during low fatigue cycle test, the metastable austenite is hardened and its fatigue life becomes shorter than that of the stable austenite. The $\gamma \rightarrow \alpha'$ transformation is then responsible for this behaviour. On the other hand, two types of martensite are observed in cold worked Fe-Ni-C alloys; the first type, stress-assisted martensite, is simply the same plate martensite that forms spontaneously below M_s except that it is somewhat finer and less regularly shaped than that formed by a temperature drop alone. The second type, strain-induced martensite, formed along the slip bands of austenite as sheaves of fine parallel laths less than $0.5 \mu\text{m}$ wide strung out on the $\{111\}$ planes of the austenite (8). The later type does not exceed 5% and forms before plate martensite (8). Figure 5 shows that in Fe-23%Ni-0.4%C both types of martensite are observed at high plastic strain amplitude, the lath martensite is observed only at low amplitude.

Hydrogen permeation in cold worked austenite phase is promoted by the mobile dislocations created during plastic deformation (9). Hydrogen atoms are swept along by the mobile dislocations, in the austenite matrix which undergoes cycle hardening due to $\gamma \rightarrow \alpha'$ transformation. These dislocations pile up on the slip bands at which strain induced martensite is initiated and on fine plates of stress assisted martensite. Figures 2a and 2b show that the same maximum stress before failure is reached at lower values of the cumulative plastic strain when the alloy is hydrogen charged than in the virgin alloy. According to CONSIDERE criterion, the strain exponent must be then lower for the hydrogenated alloy than for the alloy tested in air. This criterion is in good agreement with our results showing that $n'_H < n'_{air}$ and also with the results obtained by tensile test on AISI 304 steel (10). Cyclic hydrogen embrittlement index $F_C\%$ decreases with increasing the plastic strain amplitude, i.e. in spite of the increase of the volume fraction of α' . This means that hydrogen initiates embrittlement at slip bands at which strain-induced martensite is formed. The failure surface observed without hydrogen at high plastic strain amplitude is ductile with dimples and contains striated twins, figure 6, but this surface is completely striated at low plastic strain amplitude. The failure surface observed with hydrogen is of brittle type with cleavage and parallel cracks, figure 7. The density of these cracks increases when the plastic strain amplitude increases. The quantity of desorbed hydrogen, in spite of the high scattering, shows that the hydrogen concentration leading to embrittlement depends highly on the fatigue life, i.e. on time of hydrogen charging in the austenitic/martensite phases, in the range of plastic strain amplitudes employed.

CONCLUSION

In this work, we have studied hydrogen embrittlement in metastable austenitic Fe-23%Ni-0.4%C alloy during low cycle fatigue test. The results obtained suggest the following conclusions:

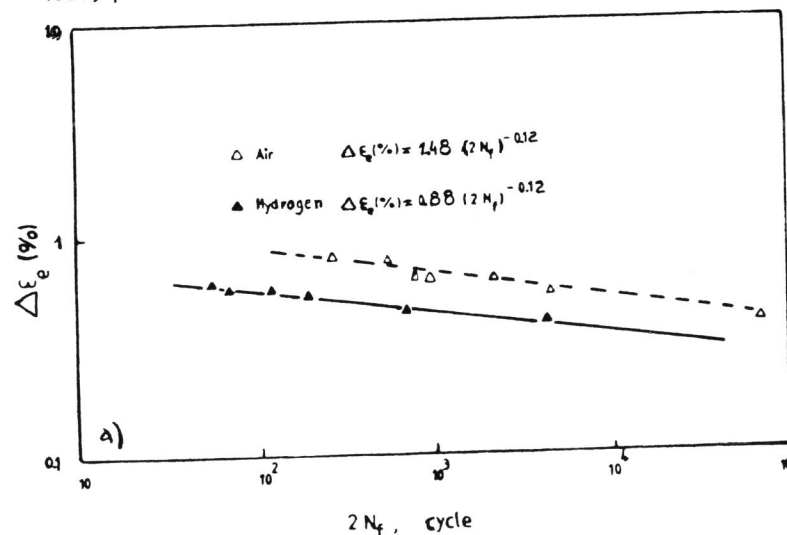
1 - The Fe-Ni-C alloy hardens during the low cycle fatigue process due to $\gamma \rightarrow \alpha'$ transformation. α' is of two types: strain-induced martensite formed at low plastic strain amplitude and stress-assisted martensite, the former one being observed at high plastic strain amplitude.

2 - Cathodic hydrogen reduces the strain hardening exponent and the cumulative plastic strain, but produces the same maximum stress, as in the case of the alloy without hydrogen, for the same plastic strain amplitude. The cyclic hydrogen embrittlement index $F_C\%$ and the amount of desorbed hydrogen at 600°C (under vacuum) both decrease with increasing plastic strain amplitude.

3 - Examination of failure surfaces shows that without hydrogen striations are presented as the mechanism of rupture at low plastic strain amplitude and that ductile rupture dominates at high plastic strain amplitude. With hydrogen, the cleaved surface with parallel cracks are observed. The results point out that $\gamma \rightarrow \alpha'$ transformation is presumed to be responsible for hydrogen embrittlement.

REFERENCES

- (1) V.F. ZACKAY, E.R. PARKER, R. BUSCH - Trans ASM, vol 60, (1967), p. 252.
- (2) F. LECROISEY, A. PINEAU - Metall. Trans., 3, (1972), p. 387.
- (3) A. PINEAU, R. PELLOUX - Metall. Trans., 5, (1974), p. 1103.
- (4) G. BAUDRY - A. PINEAU - Mater Science and Engin, 28, (1977), p. 229.
- (5) R.G. CHANANI, S.D. ANTOLOVICH - Metall. Trans., 5, (1974), p. 217.
- (6) S.S. MANSON, M.H. HIRSCHBERG - Proc. "In fatigue an interdisciplinary approach", Syracuse Univ., Press. Syracuse, N.Y. (1964), p. 133.
- (7) R.W. LANDGRAF - ASTM - STP 467, (1970), p. 3.
- (8) P.C. MAXWELL, A. GOLDBERG, J.C. SHYNE - Metall. Trans., 5, (1974), p. 1305.
- (9) J.A. DONOVAN - Metall. Trans., 7A, (1976), p. 145.
- (10) P.E.V. DE MIRANDA - Proc. of 8th Inter. Conf. of the Strength of Metals and Alloys, Pergamon Press, TAMPERE, FINLAND, August 1988, p. 1221.



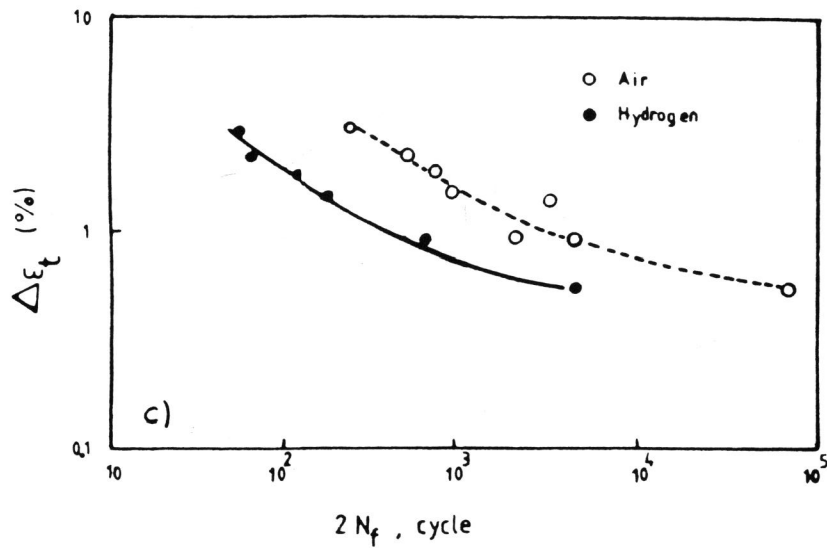
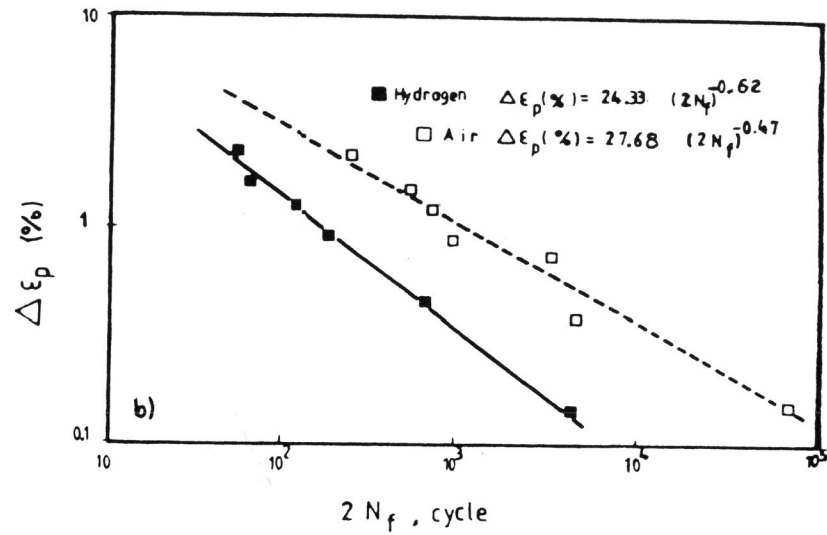


Figure 1: Effect of hydrogen on the L.C.F. behaviour.
 a - elastic resistance versus N_f
 b - plastic resistance versus N_f
 c - elastic and plastic resistances versus N_f

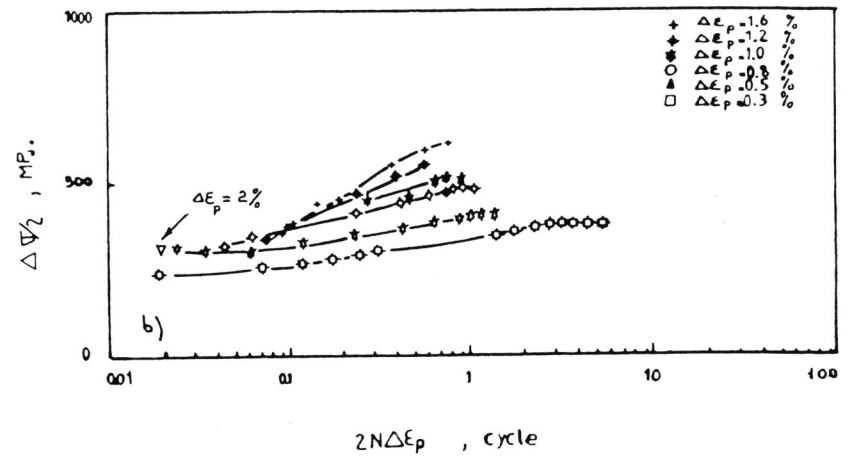
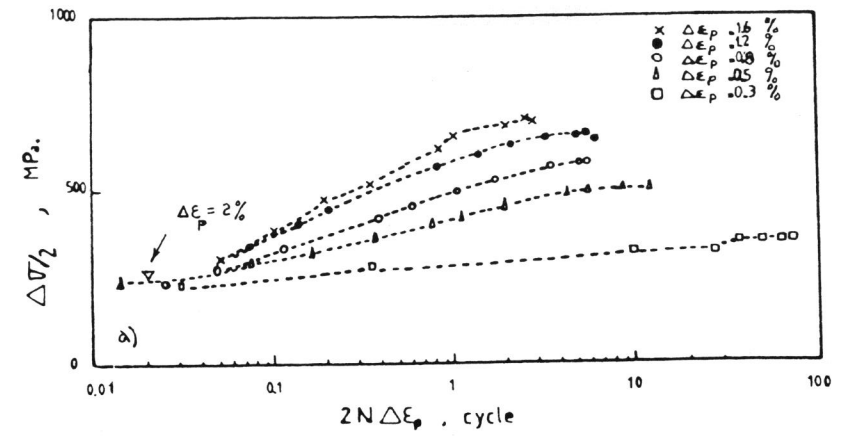


Figure 2: Variation of the hardening behaviour as a function of the cumulative plastic strain.
 a - without hydrogen
 b - with hydrogen

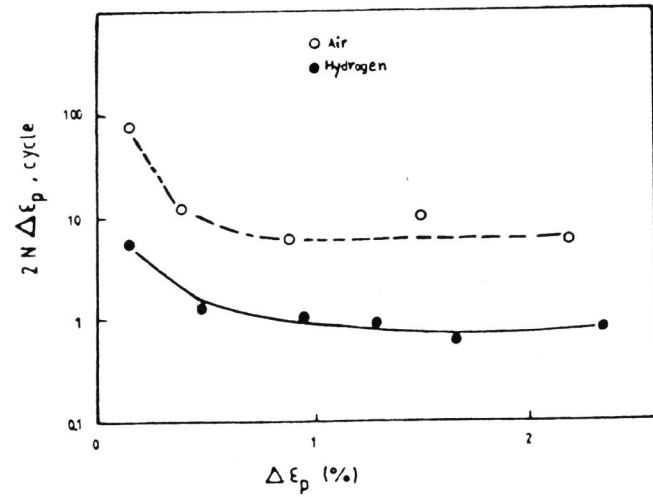


Figure 3: Cumulative plastic strain versus plastic strain amplitude; with and without hydrogen.

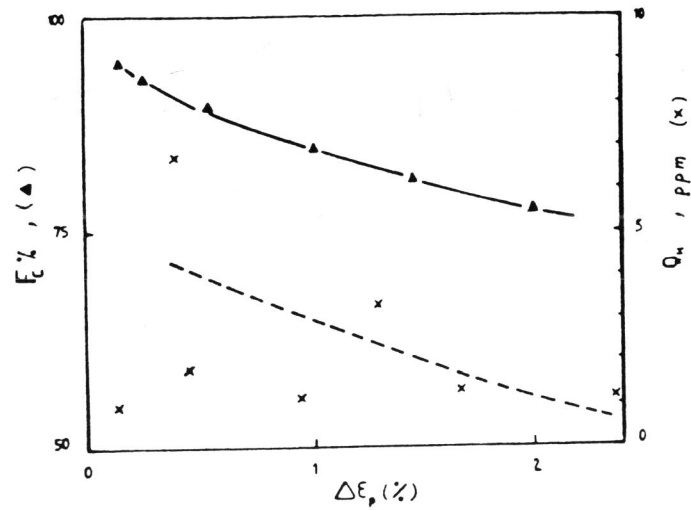


Figure 4: F_c % and Q_H variations as a function of the plastic strain amplitude.

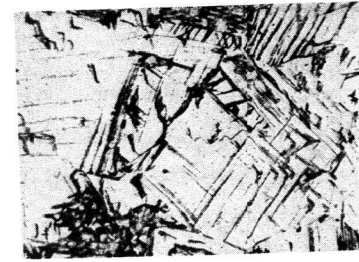


Figure 5: Stress-assisted and strain-induced martensites observed in Fe-23%Ni-0.4%C alloys. (X 144)

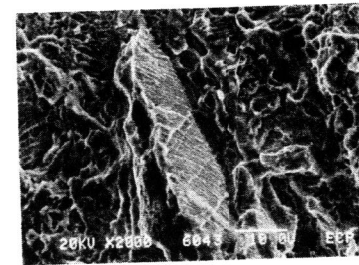


Figure 6: Failure surface observed at high plastic strain amplitude: alloy without hydrogen.

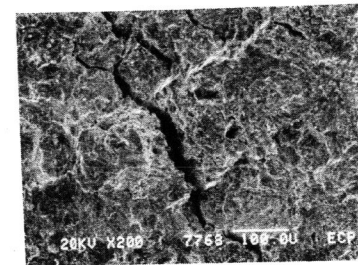


Figure 7: Failure surface observed at high plastic strain amplitude: alloy with hydrogen.